Characterizing the Influence of Preload Dosing on Percent Signal Recovery (PSR) and Cerebral Blood Volume (CBV) Measurements in a Patient Population With High-Grade Glioma Using Dynamic Susceptibility Contrast MRI

Laura C. Bell[1], Leland S. Hu[2], Ashley M. Stokes[1], Samuel C. McGee[1], Leslie C. Baxter[1], and C. Chad Quarles[1]

[1]Division of Imaging Research, Barrow Neurological Institute, Phoenix, Arizona; and [2]Department of Radiology, Mayo Clinic Arizona, Scottsdale, Arizona

Corresponding Author:
C. Chad Quarles, PhD
Barrow Neurological Institute,
350 W Thomas Rd, Phoenix, AZ 85018;
E-mail: chad.quarles@barrowneuro.org

ABSTRACT

With DSC-MRI, contrast agent leakage effects in brain tumors can either be leveraged for percent signal recovery (PSR) measurements or be adequately resolved for accurate relative cerebral blood volume (rCBV) measurements. Leakage effects can be dimished by administration of a preload dose before imaging and/or specific postprocessing steps. This study compares the consistency of both PSR and rCBV measurements as a function of varying preload doses in a retrospective analysis of 14 subjects with high-grade gliomas. The scans consisted of 6 DSC-MRI scans during 6 sequential bolus injections (0.05 mmol/kg). Mean PSR was calculated for tumor and normal-appearing white matter regions of interest. DSC-MRI data were corrected for leakage effects before computing mean tumor rCBV. Statistical differences were seen across varying preloads for tumor PSR (*P* value = 4.57E-24). Tumor rCBV values did not exhibit statistically significant differences across preloads (*P* value = .14) and were found to be highly consistent for clinically relevant preloads (intraclass correlation coefficient = 0.93). For a 0.05 mmol/kg injection bolus and pulse sequence parameters used, the highest PSR contrast between normal-appearing white matter and tumor occurs when no preload is used. This suggests that studies using PSR as a biomarker should acquire DSC-MRI data without preload. The finding that leakage-corrected rCBV values do not depend on the presence or dose of preload contradicts that of previous studies with dissimilar acquisition protocols. This further confirms the sensitivity of rCBV to preload dosing schemes and pulse sequence parameters and highlights the importance of standardization efforts for achieving multisite rCBV consistency.

INTRODUCTION

Dynamic susceptibility contrast magnetic resonance imaging (DSC-MRI)-based percent signal recovery (PSR) and relative cerebral blood volume (rCBV) measurements have been extensively researched as biomarkers to aid in diagnosis (1), assess treatment response (2, 3), obtain improved image-guided biopsies (4, 5), and to differentiate between posttreatment radiation effects (6, 7) and glioma progression (8-10). However, contrast agent (CA) extravasation is prevalent in subjects with brain cancer because of the breakdown of the blood–brain barrier (BBB), and it is known to confound reliable cerebral blood volume estimation. CA extravasation induces local T1 and T2*

leakage effects that alter the measured DSC signal intensity (SI) time curves (11-13). Postcontrast SI time points may either increase (because of T1 effects) or decrease (because of additional T2* effects) relative to precontrast time points based on these leakage effects. The magnitude and influence of these CA leakage effects on PSR and rCBV depend on image acquisition parameters (14-17), CA preload dosing (13, 18), and/or leakage-correction postprocessing methods (12, 19-21).

Preload dosing involves the injection of CA several minutes before the bolus injection used for acquisition of DSC-MRI data. The goal of preload dosing is to sufficiently decrease the local tissue T1, such that subsequent CA injections induce only minor

additional T1 changes, and thereby enhancing sensitivity to the expected T2* changes. Because of the challenges of validating rCBV measures acquired with and without preload dosing in subjects, there is considerable multisite variability, with preload doses ranging from 0.025 to 0.1 mmol/kg. Characterizing the influence of variable preload dosing on DSC-MRI-derived biomarkers is critically important because of the increasing concerns regarding the total amount of gadolinium administered in subjects and for standardization efforts aiming to identify consistent multisite acquisition protocols.

PSR relies on heterogeneous CA-induced leakage effects, and ideally, would predominantly reflect the underlying tumor physiology (vascular permeability, CA kinetics, and tissue microstructure— e.g., cell density and size). However, a prior study comparing PSR across different combinations of echo times (TE), flip angles (FA), and CA doses showed that PSR highly depends on pulse sequence parameters and preload dose (10). However, it is currently unknown how systematic increases in preload dose influence PSR when the acquisition parameters are held constant.

Unlike PSR measurements, which are computed from the raw DSC-MRI signals, reliable rCBV estimation requires the application of leakage-correction algorithms to the acquired data during postprocessing. A commonly used leakage-correction algorithm is the Boxerman–Schmainda–Weisskoff (BSW) approach (20), which assumes unidirectional CA efflux and uses DSC-MRI curves from a "whole-brain nonenhancing" region to estimate and remove T1- or T2*-based leakage effects from data measured in tumor regions of interest (ROIs). For each voxel, the magnitude of the leakage effects is quantified through the BSW parameter, $K2$, which, like PSR, is sensitive to local vascular permeability and tissue microstructure. The sign of $K2$ reflects whether the effects are T1-(positive) or T2*-(negative) based. For a given pulse sequence, it is relevant to characterize how variable preload doses influence the consistency of BSW-corrected rCBV measurements and the extracted $K2$ parameter. In a dose-dependent manner, CA preloads decrease, and potentially increase, the magnitude of T1 and T2* leakage effects, and could alter the magnitude and biophysical interpretation of $K2$.

In this study, we retrospectively analyze a unique data set, wherein 14 glioma subjects underwent 6 consecutive DSC-MRI scans during the same imaging session (7). The acquisition parameters of each DSC-MRI scan were held constant, while incremental doses of preloads were administered. This data set was originally acquired to examine the effect of preload dosing and baseline subtraction leakage correction on the potential for rCBV to differentiate posttreatment radiation effects and tumor recurrence (18). Although the pulse sequence parameters used in this retrospective study differ from the recent recommendations of the American Society of Functional Neuroradiology (22), this valuable data set enables the systematic characterization of the influence of preload dosing on T1 and T2* leakage effects and the derived PSR- and BSW-corrected rCBV parameters. Such an analysis could guide optimal PSR acquisition strategies and comparability of rCBV across subject studies where variable preload doses may be used.

MATERIALS AND METHODS

This manuscript is a retrospective analysis of data acquired, with approval from our institutional review board, from January 2007 to April 2008, with results from a separate stand-alone study published in May 2008 and January 2010 (7, 18). In summary, 14 subjects (males, 11; females, 3; average age, 57.2 ± 12.4 years) with World Health Organization grade III and IV primary high-grade gliomas undergoing preoperative imaging for surgical reresection of recurrent newly developed contrast-enhancing lesions were recruited. All subjects in this study received initial treatment (surgical resection with adjuvant chemotherapy and radiation therapy) before enrollment.

Scanning and Contrast Injection Protocol

MRI was performed on a 3 T magnetic resonance (MR) imaging system (Signa HDx; GE Healthcare, Milwaukee, Wisconsin) using a dedicated 8-channel phased-array brain coil. A standard gradient-echo echo-planar imaging DSC sequence was used with the following parameters: repetition time (TR)/TE = 2000 milliseconds/20 milliseconds, FA = 60°, field of view = 24 × 24 cm², section thickness = 5 mm, section spacing = 0 mm, number of slices = 27, and acquired matrix = 96 (frequency) × 128 (phase). An individual DSC scan time was 2 minutes with 60 time points and 1 minute of wait-time before starting the next DSC scan. Each subject was scanned with a conventional DSC sequence 6 times with a step-wise preload protocol (as outlined below).

Gadodiamide (Omniscan; Nycomed Amersham, Oslo, Norway) was hand-administered for each perfusion scan at 0.05 mmol/kg (one-half of a standard dose) at an estimated rate of 3–5 mL/s followed by a 20-mL saline flush at the same rate by an experienced neuroradiologist (LSH, 7 years of experience). To ensure reliable hand injections, the intravenous catheter was placed in the antecubital fossa of the forearm with an 18-gauge needle. The injection always occurred 20 s after the start of the DSC scan.

A total of 6 consecutive DSC scans with identical imaging parameters were acquired, each with 0.05 mmol/kg injection. Time between each DSC scan was 3 minutes (2-minute DSC scan + 1-minute wait-time) for a total imaging session of 17 minutes. Because the DSC scans were consecutively acquired, the total amount of preload before the DSC acquisition increased linearly in half-doses from 0 (preload 0–no preload) to 2.5× the standard dose (preload 5) as defined in Table 1. For a more illustrative explanation, please see Figure 1 in Hu et al.'s original manuscript (18).

Finally, the scan protocol included a postcontrast T1-weighted inversion recovery spoiled gradient echo sequence (TI/TR/TE = 300/6.8/2.8 milliseconds, field of view = 26 × 26 cm², slice thickness = 2 mm, and acquired matrix = 320 × 224) for ROI delineation during postprocessing.

Image Analysis and Postprocessing

PSR Measurements. The T1-weighted anatomical data were coregistered to the DSC perfusion data using rigid registration with FMRIB Software Library (23). The PSR measurements were performed using MATLAB (The MathWorks Inc., Natick, Massachusetts).

Table 1. Summary of Total Dose of Administered Contrast Agent in Each DSC Scan

Preload Number	Amount of Preload (mmol/kg)	Total Dose [Preload, Injection] × Standard Dose
0	None	[0.0, 0.5]
1	0.05	[0.5, 0.5]
2	0.10	[1.0, 0.5]
3	0.15	[1.5, 0.5]
4	0.20	[2.0, 0.5]
5	0.25	[2.5, 0.5]

ROI-based analysis was used to evaluate the influence of the preload dose on PSR measurements. The enhancing brain tumor was segmented on the postcontrast T1-weighted anatomical data by semiautomatic SI thresholding. To isolate the tumor from other tissues with a bright signal, a 3-dimensional region-growing technique was then applied by manually selecting the seed to occur within the tumor ROI. The normal-appearing white matter (NAWM) ROI was manually drawn by drawing a circular ROI within NAWM contralateral to the tumor location. When these 2 masks were applied to the DSC data, voxels were thresholded on the basis of the signal–time intensity curves to ensure a DSC signal drop of at least 5 standard deviations from the precontrast time points.

Before our semiquantitative measurements were calculated, we first sought to separate the T1 and T2* leakage effects as a function of preload dose within the tumor ROI. The leakage effects were arbitrarily categorized as T1-related if the postcontrast SI was 5% or greater than the precontrast SI, and T2*-related if the postcontrast SI was −5% or less than the precontrast SI. The percentage of voxels exhibiting T1 or T2* leakage effects or neither was then calculated across preloads for each subject.

Whole-brain, voxel-wise PSR values were calculated from the SI time curves as follows (10):

$$PSR = \frac{S_{post} - S_{min}}{S_{pre} - S_{min}} \times 100\% \qquad (1)$$

Where precontrast (S_{pre}) and postcontrast (S_{post}) SIs were averaged over 10 timepoints, and S_{min} is the minimum signal drop at CA arrival. The magnitude and range of PSR values in NAWM is rarely reported; however, we elected to include it in this study because it could inform interpretation of tumor data, serving as a control in tissue where the BBB is intact.

rCBV Measurements. The rCBV measurements were calculated following CA leakage correction using the BSW leakage-correction method and normalized to NAWM using the Food and Drug Administration-cleared IB Neuro software (Imaging Biometrics, LLC, Elm Grove, Wisconsin). Mean rCBV values within the tumor ROI are reported in this manuscript. In addition, the computed K2 scaling parameter (the permeability constant) maps from the BSW fit were saved alongside the rCBV maps. IB Neuro rCBV maps and K2 maps were exported to MATLAB such that the same ROIs were used between the PSR and rCBV measurements.

Statistics

To evaluate the effect of preload dosing on PSR and rCBV, the mean values of each measurement were statistically compared by performing repeated-measures one-way ANOVA, where data were grouped by preload dose. If the ANOVA test resulted in a statistical difference across preloads, post hoc pairwise comparisons adjusted for multiple comparisons using the Tukey–Kramer approach were conducted. Statistical differences were defined as a *P*-value of <.05. To evaluate the consistency in rCBV across preloads, the intraclass correlation coefficient (ICC) was calculated. All statistical tests were done in MATLAB (The MathWorks Inc.).

RESULTS

Figure 1 characterizes the amount of T1 and T2* leakage effects across preload. In general, the percentage of voxels exhibiting
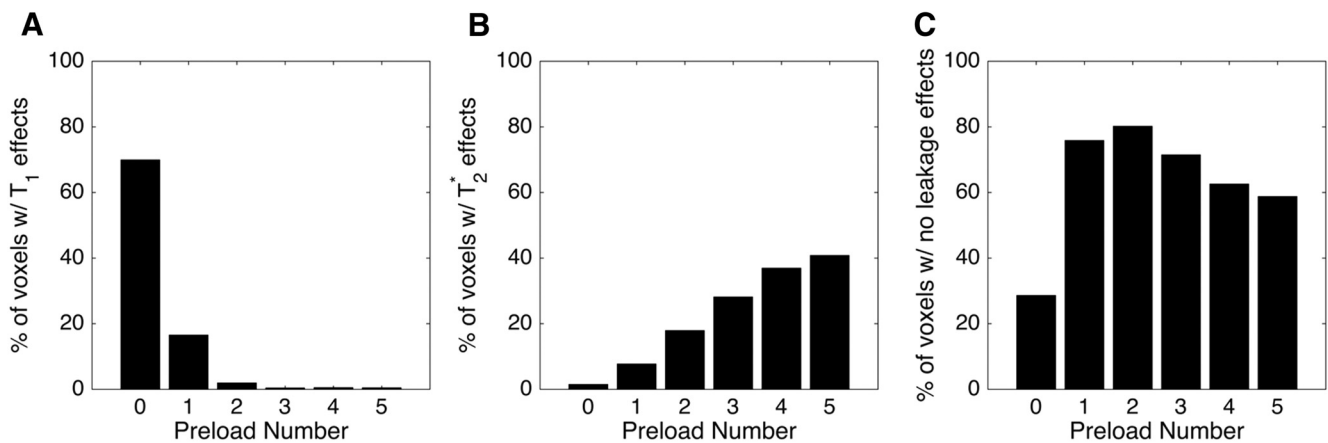

Figure 1. Percentage of tumor voxels that showed T1 leakage effects (A), T2* leakage effects (B), or no leakage effects (C) across all subjects as a function of preload dose.
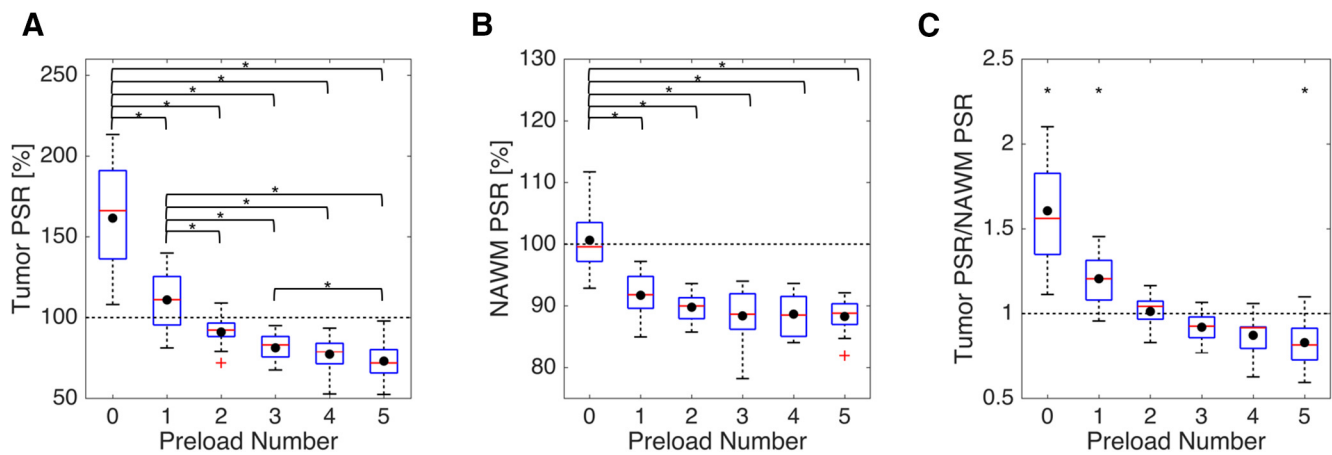
Figure 2. Boxplot representation (red line is the median; black solid dot is the mean) of tumor (A) and normal-appearing white matter (NAWM) (B) percent signal recovery (PSR) as a function of preload dose. Statistical differences (P-value <.05) between preloads are indicated by the brackets with an asterisk. The ratio of tumor PSR to NAWM PSR is represented across preloads along with an asterisk above the preload dose number if a statistical difference between tumor and NAWM PSR was observed (C).

T1 leakage effects is prominently observed in the case without preload (70%) and is substantially reduced for preload 1 (16.5%) and preloads 2–5 (<2%). In contrast, the percentage of voxels exhibiting T2* leakage effects is minimal in the case without preload (<2%) and gradually increases from preload 1 (8%) to preload 5 (40%). Total leakage effects are minimized for preloads 1 and 2, where 75%–80% of voxels exhibit no detectable leakage effects.

Figure 2 illustrates the mean PSR for both the tumor and NAWM ROIs across preloads. Tumor PSR is the greatest for no preload (preload 0), when sensitivity to T1 leakage effects is expected to be at a maximum, and decreases with increasing preload (Figure 2A). The mean tumor PSR decreases to <100% by preload 3 and remains statistically similar for preloads 4–5 (P-value >.71). Tumor PSR is statistically different across all preloads (ANOVA P-value = 4.57E-24). Specifically, statistical differences are seen in tumor PSR for preload 0 compared with that in preloads 1–5 (P-values = 2.07E-8 for all 5 comparisons). Furthermore, statistical differences are seen for preload 1 compared with preloads 3–6 (preload 1 vs. preload 3 P-value = .01; preload 1 vs preload 4 P-value = 4.74E-05; preload 1 vs. preload 5 P-value = 3.65E-06; and preload 1 vs. preload 5 P-value = 2.11E-07) and for preload 3 compared with to preload 6 (P-value = .03). The NAWM PSR follows a trend similar to that of tumor PSR, as it is the greatest at preload 0 and decreases with a preload dose (ANOVA P-value = 3.98E-17). The mean NAWM PSR, unlike that found in tumor, is relatively constant across preloads 1–5 (Figure 2B). NAWM PSR is statistically different for preload 0 compared with preloads 1–5 (P-values = 2.07E-8 for all 5 comparisons); however, it is statistically similar for all comparisons for preloads 1–5 (P-values >.05 for all 10 comparisons). The ratio of tumor PSR to NAWM PSR is presented in Figure 2C. Tumor PSR is statistically different than NAWM PSR for preload 0 (P-value = 2.24E-7), preload 1 (P-value = .0006), and preload 5 (P-value = .02). Both tumor and NAWM PSR are

similar for preloads 2–4 (preload 2 P-value = 1.00, preload 3 P-value = .90, and preload 4 P-value = .28).

Figure 3 illustrates the mean rCBV for the tumor ROI in each subject across all preload numbers (Figure 3A). No statistical differences were observed in rCBV between all comparisons for preloads 0–5 (ANOVA P-value = .144). The coefficient of variation (CV%) for each subject is included in Table 2, along with the ICC values. The coefficient of variation (CV%) and ICC are reported across all preloads (preloads 0–5 ICC = 0.81) and increases for only the clinically relevant preloads (preloads 0–2 ICC = 0.93). The mean permeability scaling factor K2 from the BSW fit are presented in a boxplot format in Figure 3B. Overall, the mean K2 values in the tumor decrease with increasing preloads and seem to remain constant for preloads 3–5. Statistical differences are seen in K2 between preload 0 compared with preloads 1–5 (preload 0 vs. preload 1 P-value = .3E-03; preload 0 vs. preload 2 P-value = .3E-03; preload 0 vs. preload 3 P-value = .3E-03; preload 0 vs. preload 4 P-value = 1.47E-05; preload 0 vs. preload 5 P-value = 1.91E-07). Furthermore, statistical differences are seen for tumor K2 values in preload 1 compared with those in preloads 3–5 (preload 1 vs. preload 3 P-value = .04; preload 1 vs. preload 4 P-value = .03; preload 1 vs. preload 5 P-value = .001). As expected, the mean K2 values in the NAWM (preload 0 = −0.004, preloads 2–5 = −0.01) are approximately equal to 0, and the only observed statistical difference was between preloads 0 and 2 (P-value = .04).

Figure 4 qualitatively displays 1 subject's PSR (top row) and rCBV (bottom row) maps for clinically relevant preload cases (preloads 0–2). Tumor PSR is clearly distinguished from the rest of the brain for the preload 0 case, but the contrast between tumor and NAWM decreases for preloads 1–2. With preload 2, the tumor PSR is visually less than NAWM PSR. The tumor rCBV maps are consistent across all preloads.
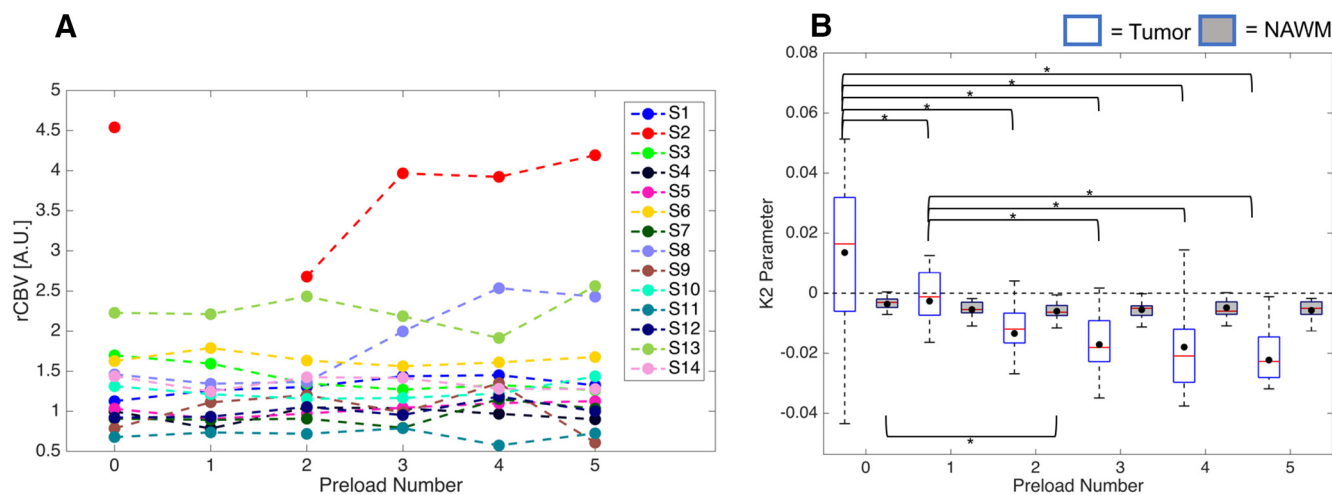
Figure 3. Mean tumor relative cerebral blood volume (rCBV) for each subject (n = 14) plotted across preload doses (A). No dynamic susceptibility contrast (DSC) signal drop was observed during the first pass of subject 2's (S2; red data points) second injection, and therefore, it was excluded from analysis. Mean K2 scaling constants (the permeability factor from the Boxerman–Schmainda–Weiskoff [BSW] fit) are represented by boxplots for both the tumor and NAWM region of interest (ROI) (B). Statistical differences (P-value <.05) between preloads are indicated by the brackets with an asterisk.

DISCUSSION

When the BBB remains intact, the dynamic CA bolus will remain in the intravascular space and DSC-MRI SI changes will predominantly reflect the CA-induced T2* changes; however, this

assumption does not always hold for imaging subjects with brain cancer. When the BBB is damaged, the dynamic CA bolus will extravasate into the extravascular space and cause local T1 and T2* leakage effects that will alter the SI time curves. The degree to which T1 and T2* leakage effects influence the acquired DSC-MRI signals depends upon the pulse sequence parameters, preload dose, CA kinetics, and the underlying tissue microstructure [24]. When developing DSC-MRI biomarkers, these leakage effects can either be exploited such as is the case with PSR measurements or need to be corrected for such as is the case with rCBV measurements. In this study, we investigated the relationship between varying amounts of preload dose on both PSR and rCBV measurements.

PSR measurements exploit the postcontrast SI which reflects competing T1 and T2* leakage effects. Boxerman et al. showed that PSR is affected by both pulse sequence parameters and CA dose for high-grade gliomas [10]. However, in this study, the pulse sequence parameters were held constant, while the preload dose was varied in a step-wise manner. Another key difference between the 2 studies is the use of a 0.05 mmol/kg injection dose, for both preload and bolus injections, instead of a standard full dose. For the clinically relevant preload cases (preloads 0, 1, and 2, representing no preload, one-half of a full dose, and a full dose preload, respectively), NAWM and tumor PSR are statistically different (except for NAWM PSR between preloads 1 and 2). This indicates that PSR cannot be compared across studies using different preload amounts, even if the pulse sequence parameters are the same. This preload-dependent PSR shows a shift in the number of voxels exhibiting T1 and T2* leakage effects that originate from dissimilar biophysical phenomena. Furthermore, tumor and NAWM PSR are only statistically different in the case of preload 0 (no preload) and preload 1, and are statistically identical for preload 2. If tumor and

Table 2. Summary of CV and ICC for Tumor rCBV Measurements

| Subject Number	CV (%): Preloads 0–5	CV (%): Preloads 0–2
S1	9.1	7.6
S2[a]	18.3	36.5
S3	12.9	11.6
S4	10.4	14.8
S5	8.0	6.6
S6	4.7	5.5
S7	13.3	1.0
S8	29.2	4.5
S9	27.1	21.1
S10	8.5	6.4
S11	10.3	4.2
S12	9.9	7.6
S13	9.9	5.4
S14	6.5	7.8
ICC[b]	0.81	0.93

Note: Middle column indicates all preloads, and the right column indicates clinically relevant preloads.
[a]CV was calculated by excluding data from preload 1.
[b]ICC excludes all of S2 values explained in the article.
Abbreviations: CV, coefficient of variation; ICC, Intraclass correlation coefficient; rCBV, relative cerebral blood volume.

Figure 4. A qualitative illustration of PSR maps (top row) and rCBV maps (bottom row) for the 3 clinically relevant preload doses (preload 0–2 from left to right) in subject 10. The T1-weighted anatomical image is also shown without an overlay.
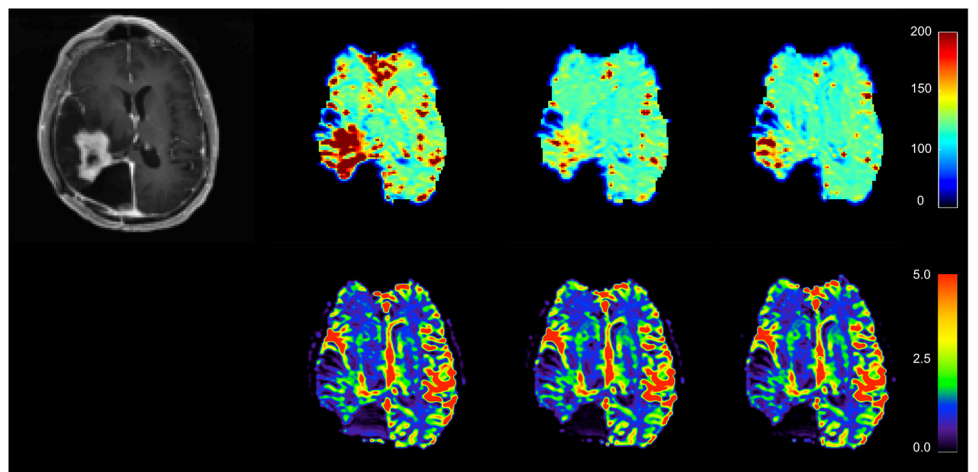
NAWM PSR are indistinguishable, as in the case of preload 2, then this would suggest that PSR-based conclusions about the underlying microstructure will be confounded. The PSR contrast between tumor and NAWM is the highest when there is no preload, indicating that this biomarker would best be measured during the initial preload administration before the bolus injection used for rCBV estimation.

Unlike PSR measurements, rCBV measurements must be corrected for T1 and T2* leakage effects to be of clinical value. In this study, we have applied the BSW leakage-correction method to our data before rCBV is calculated. Across preloads, we observed differences in mean tumor K2 values because of differing amounts of T1 and T2* leakage effects. This finding indicates that K2 as a permeability biomarker is dependent on the preload amount. When rCBV is corrected for these CA leakage effects, our results indicate that tumor rCBV is not statistically different across varying preloads including the no preload option. Furthermore, the ICC value increases from 0.81 to 0.93 for the clinically relevant preload cases, showing that rCBV across preloads is indeed consistent. It is quite compelling that the BSW correction could yield highly consistent rCBV values across preload doses given the significant change in the fraction of voxels exhibiting T1 and T2* leakage effects. This indicates that, for the pulse sequence parameters used in this study, if a half-dose of the CA is used for the bolus injection, there is no added benefit of using a preload beforehand if leakage correction is applied. It should be noted that these results do not inform on the accuracy of the derived rCBV measures or how they would compare, with respect to consistency or accuracy, to studies using full-dose bolus injections. For example, these results contradict an animal study that used a full dose (0.1 mmol/kg) and pulse sequence parameters with more T1 weighting (13). Specifically, the agreement between leakage-corrected rCBV values, acquired using a gadolinium-based agent and a reference intravascular iron-oxide agent, significantly improved with preload dose. This discrepancy further confirms the sensitivity of rCBV to pulse sequence and preload dosing protocols, as shown in a recent simulation study (25). Specifically, Leu et al. found that similar rCBV values are obtained using the ASFNR (The American Society of Functional Neuroradiology)-recommended protocol, which includes preload dosing, and those that are acquired using a pulse sequence with less T1 weighting (e.g., FA = 35°) but do not use a preload. Future studies are warranted given our results and the competing interests to reduce total CA dose versus maintaining the higher contrast to noise afforded by full-dose bolus injections, directly affecting CBV precision. It would be highly compelling to validate, in humans, whether an optimal pulse sequence protocol exists that would alleviate the need for preload dosing, as this would simplify injection protocols in subjects, reduce variability across sites, and maintain a high contrast to noise.

Despite the unique nature of this retrospective data set, there were several limitations. First, the injections in these DSC scans were hand-administered by an experienced neuroradiologist instead of using a power injector. From experience, our neuroradiologist used slightly larger-gauge intravenous catheters for the injections to help control the injection bolus. Furthermore, upon inspection during postprocessing for this study, we qualitatively observed highly consistent arterial input functions chosen by an automatic algorithm (results not shown) across preloads for each subject. Consistency in the arterial input function made us more confident about our experienced neuroradiologist hand-administering the injections. Second, as noted above, the results of this study are specific to pulse sequence parameters used for DSC-MRI acquisition, particularly as TR, TE and FA can alter a signal's sensitivity to T1 and T2* leakage effects. Compared with the recent ASFNR recommendations, the 2-second TR used in this study is longer than the recommended 1.5 seconds. At the time of the study, a longer TR was chosen for sufficient brain coverage. With the recommended 1.5-second TR, the PSR magnitude would increase because of the elevated T1 weighting, but the changes in PSR across preloads would remain the same. For example, the percent of voxels exhibiting T1 leakage effects (Figure 1A) would be slightly increased than that reported; however, the T1 leakage effects would still decrease with increasing preload dose. Third, the results presented are pertinent for a 0.05 mmol/kg injection bolus dosage, which is a common option in the clinic. Although our results show that tumor rCBV is similar for preload dose options including "no preload," this preload dosing result might not apply for a full standard-dose injection. A full standard dose could also shift the sensitivity of the acquired data to T1 and T2* leakage effects.

In conclusion, we have shown that, with the acquisition parameters used herein, PSR measurements vary across preload amounts, whereas rCBV measurements do not. Specifically, tumor PSR measurements differed for preload 0 (no preload), preload 1 (0.05 mmol/kg), and preload 2 (0.1 mmol/kg). Furthermore, tumor PSR was found to be similar to NAWM PSR for preload 2, indicating that the highest contrast for PSR maps can be achieved with preload 0 and, to a smaller degree, preload 1.

However, PSR measurements with different preload CA doses cannot be compared across studies. Tumor rCBV values were shown not to be statistically different across preloads, indicating that future studies should seek to establish whether pulse sequence parameters can be optimized such that preload dosing can be eliminated without affecting rCBV accuracy. The results of this study also justify standardization efforts for DSC-MRI, which are critically important for achieving multisite rCBV consistency.

REFERENCES

1. Fink JR, Muzi M, Peck M, Krohn KA. Multimodality brain tumor imaging: MR imaging, PET, and PET/MR imaging. J Nucl Med. 2015;56(10):1554–1561.
2. Boxerman JL, Ellingson BM, Jeyapalan S, Elinzano H, Harris RJ, Rogg JM, Pope WB, Safran H. Longitudinal DSC-MRI for distinguishing tumor recurrence from pseudoprogression in patients with a high-grade glioma. Am J Clin Oncol. 2014 [Epub ahead of print].
3. Ellingson BM, Zaw T, Cloughesy TF, Naeini KM, Lalezari S, Mong S, Lai A, Nghiemphu PL, Pope WB. Comparison between intensity normalization techniques for dynamic susceptibility contrast (DSC)-MRI estimates of cerebral blood volume (CBV) in human gliomas. J Magn Reson Imaging. 2012;35(6):1472–1477.
4. Chaskis C, Stadnik T, Michotte A, Van Rompaey K, D'Haens J. Prognostic value of perfusion-weighted imaging in brain glioma: a prospective study. Acta Neurochir (Wien). 2006;148(3):277–285.
5. Maia AC Jr, Malheiros SM, da Rocha AJ, Stávale JN, Guimarães IF, Borges LR, Santos AJ, da Silva CJ, de Melo JG, Lanzoni OP, Gabbai AA, Ferraz FA. Stereotactic biopsy guidance in adults with supratentorial nonenhancing gliomas: role of perfusion-weighted magnetic resonance imaging. J Neurosurg. 2004;101(6):970–976.
6. Barajas RF Jr, Chang JS, Segal MR, Parsa AT, McDermott MW, Berger MS, Cha S. Differentiation of recurrent glioblastoma multiforme from radiation necrosis after external beam radiation therapy with dynamic susceptibility-weighted contrast-enhanced perfusion MR imaging. Radiology. 2009;253(2):486–496.
7. Hu LS, Baxter LC, Smith KA, Feuerstein BG, Karis JP, Eschbacher JM, Coons SW, Nakaji P, Yeh RF, Debbins J, Heiserman JE. Relative cerebral blood volume values to differentiate high-grade glioma recurrence from posttreatment radiation effect: direct correlation between image-guided tissue histopathology and localized dynamic susceptibility-weighted contrast-enhanced perfusion MR imaging measurements. AJNR Am J Neuroradiol. 2009;30(3):552–558.
8. Danchaivijitr N, Waldman AD, Tozer DJ, Benton CE, Brasil Caseiras G, Tofts PS, Rees JH, Jäger HR. Low-grade gliomas: do changes in rCBV measurements at longitudinal perfusion-weighted MR imaging predict malignant transformation? Radiology. 2008;247(1):170–178.
9. Rossi Espagnet MC, Romano A, Mancuso V, Cicone F, Napolitano A, Scaringi C, Minniti G, Bozzao A. Multiparametric evaluation of low grade gliomas at follow-up: comparison between diffusion and perfusion MR with ¹⁸F-FDOPA PET. Br J Radiol. 2016;89(1066):20160476.
10. Boxerman JL, Paulson ES, Prah MA, Schmainda KM. The effect of pulse sequence parameters and contrast agent dose on percentage signal recovery in DSC-MRI: implications for clinical applications. AJNR. AJNR Am J Neuroradiol. 2013; 34(7):1364–1369.
11. Weisskoff RM, Boxerman JL, Sorensen AG, Kulke STC RB. Simultaneous blood volume and permeability mapping using a single Gd-based contrast injection. In: Proceedings of the Second Annual Meeting of Society of Magnetic Resonance. San Francisco, USA; 1994.
12. Schmainda KM, Rand SD, Joseph AM, Lund R, Ward BD, Pathak AP, Ulmer JL, Badruddoja MA, Krouwer HG. Characterization of a first-pass gradient-echo spin-echo method to predict brain tumor grade and angiogenesis. AJNR Am J Neuroradiol. 2004;25(9):1524–1532.
13. Boxerman JL, Prah DE, Paulson ES, Machan JT, Bedekar D, Schmainda KM. The role of preload and leakage correction in gadolinium-based cerebral blood

volume estimation determined by comparison with MION as a criterion standard. AJNR Am J Neuroradiol. 2012;33(6):1081–1087.
14. Newbould RD, Skare ST, Jochimsen TH, Alley MT, Moseley ME, Albers GW, Bammer R. Perfusion mapping with multiecho multishot parallel imaging EPI. Magn Reson Med. 2007;58(1):70–81.
15. Paulson ES, Schmainda KM. Comparison of dynamic susceptibility-weighted contrast-enhanced MR methods: recommendations for measuring relative cerebral blood volume in brain tumors. Radiology. 2008;249(2):601–613.
16. Sourbron S, Heilmann M, Biffar A, Walczak C, Vautier J, Volk A, Peller M. Bolus-tracking MRI with a simultaneous T1- and T2*-measurement. Magn Reson Med. 2009;62(3):672–681.
17. Stokes AM, Semmineh N, Quarles CC. Validation of a T1 and T2* leakage correction method based on multiecho dynamic susceptibility contrast MRI using MION as a reference standard. Magn Reson Med. 2015;76(2):613–625.
18. Hu LS, Baxter LC, Pinnaduwage DS, Paine TL, Karis JP, Feuerstein BG, Schmainda KM, Dueck AC, Debbins J, Smith KA, Nakaji P, Eschbacher JM, Coons SW, Heiserman JE. Optimized preload leakage-correction methods to improve the diagnostic accuracy of dynamic susceptibility-weighted contrast-enhanced perfusion MR imaging in posttreatment gliomas. AJNR Am J Neuroradiol. 2010; 31(1):40–48.
19. Bjornerud A, Sorensen AG, Mouridsen K, Emblem K. T1- and T2*-dominant extravasation correction in DSC-MRI: part I–theoretical considerations and implications for assessment of tumor hemodynamic properties. J Cereb Blood Flow Metab. 2011;31(10):2041–2053.
20. Boxerman JL, Schmainda KM, Weisskoff RM. Relative cerebral blood volume maps corrected for contrast agent extravasation significantly correlate with glioma tumor grade, whereas uncorrected maps do not. Am J Neuroradiol. 2006; 27(4):859–867.
21. Leu K, Boxerman JL, Lai A, Nghiemphu PL, Pope WB, Cloughesy TF, Ellingson BM. Bidirectional contrast agent leakage correction of dynamic susceptibility contrast (DSC)-MRI improves cerebral blood volume estimation and survival prediction in recurrent glioblastoma treated with bevacizumab. J Magn Reson Imaging. 2016;44(5):1229–1237.
22. Welker K, Boxerman J, Kalnin A, Kaufmann T, Shiroishi M, Wintermark M; American Society of Functional Neuroradiology MR Perfusion Standards and Practice Subcommittee of the ASFNR Clinical Practice Committee. ASFNR recommendations for clinical performance of MR dynamic susceptibility contrast perfusion imaging of the brain. AJNR Am J Neuroradiol. 2015;36(6): E41–E51.
23. Woolrich MW, Jbabdi S, Patenaude B, Chappell M, Makni S, Behrens T, Beckmann C, Jenkinson M, Smith SM. Bayesian analysis of neuroimaging data in FSL. Neuroimage. 2009;45(1):S173–S186.
24. Semmineh NB, Xu J, Skinner JT, Xie J, Li H, Ayers G, Quarles CC. Assessing tumor cytoarchitecture using multiecho DSC-MRI derived measures of the transverse relaxivity at tracer equilibrium (TRATE). Magn Reson Med. 2015;74(3):772–784.
25. Leu K, Boxerman JL, Ellingson BM. Effects of MRI protocol parameters, preload injection dose, fractionation strategies, and leakage correction algorithms on the fidelity of dynamic-susceptibility contrast MRI estimates of relative cerebral blood volume in gliomas. AJNR Am J Neuroradiol. 2017;38(3):478–484.